Inputs and Outputs definition for the linear gyrokinetic database GKDB

Y. Camenen on behalf of the GKDB working group

Last update: March 24, 2017

Chapter 1

Preamble

This document summarises the names, conventions and normalisations adopted for the inputs and outputs of the linear gyrokinetic database (GKDB) storing results from δf, flux-tube gyrokinetic simulations.

The normalised inputs and outputs are independent of ρ^* consistently with the local approximation and a spectral representation is assumed in the perpendicular plane (i.e. homogeneous turbulence).

S.I. units are used everywhere with the exception of temperatures given in eV. This means that kT is noted T as is customary in plasma physics (and possibly confusing).

Chapter 2

Conventions and normalisations

2.1 Cylindrical and flux coordinate systems

The ITER coordinate convention is adopted for the GKDB. The corresponding index in the COordinate COnventionS system [1] is COCOS=11.

2.1.1 Cylindrical coordinate system (R, φ, Z)

A right-handed cylindrical coordinate system (R, φ, Z), with R the major radius, Z the elevation and φ the toroidal angle (increasing when anticlockwise from above) is used to describe the flux surfaces, see Fig. 2.1. The magnetic equilibrium is assumed to be axisymmetric and the poloidal contours of the flux surface $\Psi(R, Z) = \Psi_0$, with Ψ the poloidal magnetic flux, are noted $\{R_{\Psi_0}, Z_{\Psi_0}\}$.

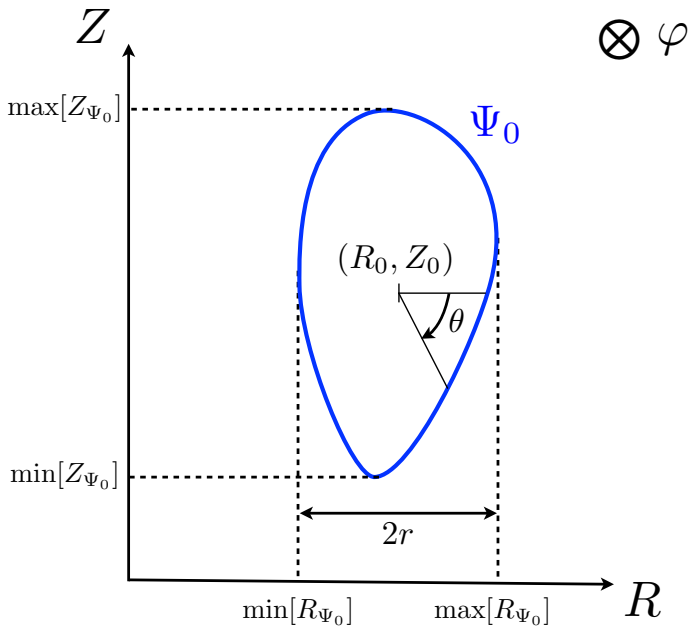

Figure 2.1: Coordinate conventions used in the GKDB (COCOS=11, [1]).

2.1.2 Flux coordinate system (r, θ, φ)

A right handed flux coordinate system (r, θ, φ) is now introduced.

Flux surface center

To start with, a reference point (R_0, Z_0) is defined for the flux surface of interest $\{R_{\Psi_0}, Z_{\Psi_0}\}$:

$$R_0 = \frac{1}{2}\left[\max[R_{\Psi_0}] + \min[R_{\Psi_0}]\right] \tag{2.1}$$

$$Z_0 = \frac{1}{2}\left[\max[Z_{\Psi_0}] + \min[Z_{\Psi_0}]\right] \tag{2.2}$$

$$\tag{2.3}$$

The reference point (R_0, Z_0) will be used in the following to define the poloidal angle. Note that (R_0, Z_0) is not the position of the magnetic axis, although it can be in some particular cases.

Radial coordinate

The radial coordinate r is defined as

$$r = \frac{1}{2}\left[\max[R_{\Psi_0}] - \min[R_{\Psi_0}]\right] \tag{2.4}$$

It has the dimension of a length and is constant on a flux surface, by definition. The radial coordinate of the flux surface $\Psi = \Psi_0$ is noted r_0.

Poloidal angle

The poloidal angle is defined from the following relationships:

$$\cos\theta = \frac{R_{\Psi_0} - R_0}{\left[(R_{\Psi_0} - R_0)^2 + (Z_{\Psi_0} - Z_0)^2\right]^{1/2}} \tag{2.5}$$

$$\sin\theta = -\frac{Z_{\Psi_0} - Z_0}{\left[(R_{\Psi_0} - R_0)^2 + (Z_{\Psi_0} - Z_0)^2\right]^{1/2}} \tag{2.6}$$

The poloidal angle is zero at the low field side midplane (the midplane is defined with respect to the flux surface $\Psi = \Psi_0$ and corresponds to $Z = Z_0$) and increases clockwise when the tokamak vertical axis is on the left of the flux surface, see Fig. 2.1.

2.2 Flux surface average

In a few cases, flux surface averaged quantities will be required. We adopt here the flux surface average definition that arises when taking the integral of a conservation equation over the volume enclosed by a flux surface (i.e. the standard procedure to built 1D transport equations in tokamaks, see for instance [2]).
The flux surface average of a quantity A is then given by

$$< A >= \frac{\int A(\mathbf{x})\delta(r - r_0)\,\mathrm{d}^3x}{\int \delta(r - r_0)\,\mathrm{d}^3x} \tag{2.7}$$

where r_0 is the radial coordinate of the flux surface on which the average is being performed, r is the value of the radial coordinate at position $\mathbf{x}$, δ is the Dirac function and the integral is being performed over the whole plasma volume (or entire world, it does not matter).
Noting that the surface element $\mathrm{d}S$ on a flux surface is related to the volume element d^3x by

$$\mathrm{d}^3x = \mathrm{d}S\frac{\mathrm{d}r}{|\nabla r|} \tag{2.8}$$

with r an arbitrary flux surface label (taken here to be the radial coordinate defined above), a convenient alternative (and equivalent) expression for the flux surface average is obtained:

$$< A >= \frac{1}{V'} \oint A \frac{\mathrm{d}S}{|\nabla r|} \tag{2.9}$$

with $V' = \frac{\partial V}{\partial r}$ and V being the volume enclosed by the flux surface labelled by r.

2.3 Normalisations

All quantities in the database (inputs and outputs) are normalised with respect to the reference quantities introduced in this section. Six reference quantities are first introduced (fundamental reference quantities) and then used to built other convenient normalising factors (derived reference quantities).
In principle, reference quantities do not need to be specified, as the purpose of the database is to relate normalised inputs to normalised outputs. However, if the choice of reference quantities is left arbitrary, the same physical inputs could lead to different normalised inputs in the database depending on the normalisation choice. This is not desirable and the reference quantities are therefore imposed.

2.3.1 Fundamental reference quantities

The six fundamental reference quantities are:

- $q_{\mathrm{ref}} = e = 1.6022 \times 10^{-19}\,\mathrm{C}$, the positive elementary charge
- $m_{\mathrm{ref}} = m_D = 3.3445 \times 10^{-27}\,\mathrm{kg}$, the Deuterium mass
- $T_{\mathrm{ref}} = T_e(r_0, \theta = 0)$, the electron temperature at $\theta = 0$
- $n_{\mathrm{ref}} = n_e(r_0, \theta = 0)$, the electron density at $\theta = 0$
- $L_{\mathrm{ref}} = R_0$, the reference length
- $B_{\mathrm{ref}} = B_t(R_0)$, the reference magnetic field (toroidal magnetic field at the flux surface center)

2.3.2 Derived reference quantities

For convenience, the following reference quantities are defined:

- $v_{\mathrm{thref}} = \sqrt{\frac{2T_{\mathrm{ref}}}{m_{\mathrm{ref}}}}$, the reference thermal velocity
- $\rho_{\mathrm{ref}} = \frac{m_{\mathrm{ref}} v_{\mathrm{thref}}}{q_{\mathrm{ref}} B_{\mathrm{ref}}}$, the reference Larmor radius

Chapter 3

Inputs

3.1 Species

For each species s, the background distribution function is supposed to be a local Maxwellian. Poloidal asymmetry in the background induced by centrifugal effects is allowed. Poloidally asymmetric quantities are given in input at $\theta = 0$. Poloidal asymmetry induced by anisotropic temperatures is not included yet, but could be introduced if need be.
At this stage, the database only stores runs with kinetic electron species (adiabatic electrons not allowed). An arbitrary number of kinetic species is allowed, but quasineutrality has to be ensured.

3.1.1 Charge

$$Z_{sN} = \frac{q_s}{q_{\text{ref}}}$$

3.1.2 Mass

$$m_{sN} = \frac{m_s}{m_{\text{ref}}}$$

3.1.3 Density

$$n_{sN} = \frac{n_s}{n_{\text{ref}}}$$

3.1.4 Logarithmic density gradient

$$L_{\text{ref}}/L_{n_s} = -L_{\text{ref}} \frac{1}{n_s} \frac{\partial n_s}{\partial r}$$

Positive for peaked profiles.

3.1.5 Temperature

$$T_{sN} = \frac{T_s}{T_{\text{ref}}}$$

3.1.6 Logarithmic temperature gradient

$$L_{\mathrm{ref}}/L_{T_s} = -L_{\mathrm{ref}}\frac{1}{T_s}\frac{\partial T_s}{\partial r}$$

Positive for peaked profiles.

3.1.7 Toroidal velocity

$$u_N = \frac{L_{\mathrm{ref}}}{v_{\mathrm{thref}}}\omega_\Phi$$

Positive for a flow in the direction of $\nabla\varphi$.
All species are assumed to have a purely toroidal flow $\mathbf{v}_s = R^2\omega_\Phi\nabla\varphi$ with a common toroidal angular frequency proportional to the background electric field:

$$\omega_\Phi = -s_j\frac{1}{|\nabla\Psi|}\frac{\partial\Phi}{\partial r},$$

with Φ the background electrostatic potential. This assumption is consistent with the ordering used in local gyrokinetic codes, as ω_Φ is the lowest order flow in a ρ_* expansion according to neoclassical theory [3].

3.1.8 Toroidal velocity gradient

$$u'_{sN} = -\frac{L_{\mathrm{ref}}^2}{v_{\mathrm{thref}}}\frac{\partial\omega_{\varphi,s}}{\partial r}$$

Positive for peaked profiles of a flow in the direction of $\nabla\varphi$.
Note that the possibility to have a species dependent toroidal velocity gradient with $\omega_{\varphi,s} \neq \omega_\Phi$ is retained. Strictly speaking, this is inconsistent with the local limit assumption $\rho_* \to 0$ but can be interesting for the interpretation of the experiments (see the discussion in section II of [4] for more details).

3.1.9 Summary of the species parameters

Name	Value/Range	Type	Dimension
charge	-	Integer	1
mass	> 0	Real	1
density	≥ 0	Real	1
density_log_gradient	-	Real	1
temperature	> 0	Real	1
temperature_log_gradient	-	Real	1
toroidal_velocity	-	Real	1
toroidal_velocity_gradient	-	Real	1

All parameters above are species dependent, except the toroidal velocity that is common to all species.

3.2 Magnetic equilibrium

The magnetic equilibrium in the vicinity of the flux surface of interest is specified by the parameters described in this section, given at $r = r_0$.

3.2.1 Radial position

$$r_N = \frac{r_0}{L_{\mathrm{ref}}}$$

3.2.2 Toroidal field direction

$$s_b = \text{sign}[\mathbf{B} \cdot \nabla\varphi]$$

3.2.3 Toroidal current direction

$$s_j = \text{sign}[\mathbf{j} \cdot \nabla\varphi]$$

with j the plasma current density. For the conventions adopted in this document, positive plasma current implies positive poloidal magnetic field.

3.2.4 Safety factor

$$q = \frac{1}{2\pi} \int_0^{2\pi} \frac{\mathbf{B} \cdot \nabla\varphi}{\mathbf{B} \cdot \nabla\theta} \, \mathrm{d}\theta$$

Note that q can be positive or negative, its sign depends on the sign of the toroidal plasma current and magnetic field:

$$q = s_b s_j |q|$$

3.2.5 Magnetic shear

$$\hat{s} = \frac{r}{q} \frac{\partial q}{\partial r}$$

3.2.6 Pressure gradient

$$\beta'_N = -\frac{2\mu_0 L_{\text{ref}}}{B^2_{\text{ref}}} \frac{\partial p}{\partial r}$$

with p the total plasma pressure (i.e. the pressure term entering the Grad-Shafranov equation). β'_N is a quantity related to the magnetic equilibrium and does not need to be consistent with the gradients (L_{ref}/L_{n_s}, L_{ref}/L_{T_s}) specified for the kinetic species.
Note that the low β' approximation for the curvature drift, i.e. the approximation

$$\mathbf{b} \times (\mathbf{b} \cdot \nabla\mathbf{n}) = \frac{1}{2}\mathbf{b} \times \nabla r \frac{2\mu_0}{B^2} \frac{\partial p}{\partial r} + \frac{\mathbf{B} \times \nabla B}{B^2} \sim \frac{\mathbf{B} \times \nabla B}{B^2},$$

is not allowed in the database as it is inconsistent with the use of a finite β'_N for the equilibrium description.

3.2.7 Plasma shape

A general description of local magnetic equilibria particularly convenient for gyrokinetic codes was introduced by J. Candy in [5]. It is used in the GKDB with a few minor modifications. The plasma shape is described by specifying the distance of the constant poloidal flux contours to the reference point (R_0, Z_0) normalised to L_{ref}:

$$a_N(r,\theta) = \frac{1}{L_{\text{ref}}} \sqrt{\left[R_\Psi(r,\theta) - R_0\right]^2 + \left[Z_\Psi(r,\theta) - Z_0\right]^2} \tag{3.1}$$

To allow regressions in the database the flux surface contours are parametrised as

$$a_N(r,\theta) = \sum_{n=0}^{N_{sh}} c_n \cos(n\theta) + s_n \sin(n\theta) \tag{3.2}$$

The specification of the local magnetic equilibrium then requires $4N_{sh} + 2$ terms, given at $r = r_0$, where N_{sh} is the degree of the expansion: $\{c_n, s_n, \frac{\partial c_n}{\partial r_N}, \frac{\partial s_n}{\partial r_N}\}$. Typically $N_{sh} \leq 8$ is sufficient to capture most of the plasma shapes but higher values can be used when needed.

3.2.8 Summary of the shape parameters

Name	Value/Range	Type	Dimension
r_minor	$0 \leq r_N \leq 1$	Real	1
ip_sign	± 1	??	1
b_field_tor_sign	± 1	??	1
q	-	Real	1
magnetic_shear	-	Real	1
beta_gradient	-	Real	1
c	-	Real	$N_{sh}+1$
dc_dr_minor	-	Real	$N_{sh}+1$
s	-	Real	N_{sh}
ds_dr_minor	-	Real	N_{sh}

3.3 Modes

As almost every gyrokinetic codes use a different coordinate system, it is convenient to specify the Fourier modes in a coordinate free form.
To define this coordinate free form, let's first call, x and y, the radial and binormal coordinates used in gyrokinetic codes to describe the turbulence in the plane perpendicular to the magnetic field. The radial coordinate x is assumed to be a flux label (i.e. $\mathbf{B}\cdot\nabla x = 0$). In a spectral representation, perturbed quantities are then written:

$$f(x,y,\theta) = \sum_{k_x,k_y} \hat{f}(k_x,k_y,\theta)\exp[ik_x x + ik_y y] \tag{3.3}$$

where θ is used as the parallel coordinate. For a given mode, the perpendicular wave vector (in real space) is given by:

$$k_\perp^2(\theta) = k_x^2 g^{xx} + 2k_x k_y g^{xy} + k_y^2 g^{yy} \tag{3.4}$$

with the code dependent metric elements given by $g^{ij} = \nabla i \cdot \nabla j$. All the metric information is on the right hand side of the equation above, the resulting $k_\perp$ does not depend on the specific coordinate choices made in gyrokinetic codes.

3.3.1 Radial mode number

The normalised coordinate independent radial mode number is defined as

$$k_{r*}\rho_{\text{ref}} = k_x\sqrt{g^{xx}(\theta=0)}\rho_{\text{ref}} \tag{3.5}$$

3.3.2 Binormal mode number

The normalised coordinate independent binormal mode number is defined as

$$k_{\theta*}\rho_{\text{ref}} = k_y\sqrt{g^{yy}(\theta=0)}\rho_{\text{ref}} \tag{3.6}$$

An alternative convenient specification of the binormal mode number is the effective poloidal mode number normalised to the ion Larmor radius $nq\rho_{\text{ref}}/r_0$ [6]. This definition is also coordinate independent and related to a physical quantity. It will not be used here as there is no simple equivalent to specify the radial wave vector.

3.4 Number of poloidal turns

In the spectral representation of a flux-tube domain, the periodicity of the torus in the poloidal direction leads to the coupling of radial modes in the parallel direction:

$$\hat{f}(k_x, k_y, \theta - \pi) = \hat{f}(k_x + \Delta k_x, k_y, \theta + \pi)$$

with Δk_x depending on the magnetic shear.
A flux-tube extending over an odd number N_p of poloidal turns with 1 radial mode k_x is therefore equivalent to a flux-tube extending over 1 poloidal turn with N_p coupled radial modes $k_x + p\Delta k_x$ with p an integer varying from $-(N_p - 1)/2$ to $(N_p + 1)/2$.
In practice, running with a sufficiently high number of poloidal turns (or coupled radial modes) is necessary to get a result independent of the boundary condition imposed at the end of the field line (when the number of poloidal turns increases, $k_\perp$ increases and the perturbations are damped by FLR effects).

3.4.1 Summary of the mode parameters

Name	Value/Range	Type	Dimension
radial_wavevector	-	Real	1
binormal_wavevector	≥ 0	Real	1
number_poloidal_turns	> 0	Integer	1

3.5 Electromagnetic effects

3.5.1 Plasma beta

The strength of the electromagnetic effects depends on the ratio of the plasma pressure to the magnetic energy and is specified by the dimensionless ratio:

$$\beta_{eN} = 2\mu_0 \frac{n_{\text{ref}} T_{\text{ref}}}{B_{\text{ref}}^2} \tag{3.7}$$

When $\beta_{eN} = 0$, the run is electrostatic.

3.5.2 Switches

- Are the fluctuations of the parallel electromagnetic vector potential $A_\parallel$ retained (magnetic field flutter)?
- Are the fluctuations of the perpendicular electromagnetic vector potential retained (magnetic field compression)?

3.5.3 Summary of the electromagnetic effects parameters

Name	Value/Range	Type	Dimension
beta	≥ 0	Real	1
a_parallel_flag	0 or 1	Logical	1
b_field_parallel_flag	0 or 1	Logical	1

3.6 Collisions

3.6.1 Plasma collisionality

The normalised collision frequency

$$\nu_{eN} = \frac{q_{\text{ref}}^2}{16\pi\epsilon_0} \frac{R_{\text{ref}} n_{\text{ref}}}{T_{\text{ref}}^2} \tag{3.8}$$

is used to specify the plasmas collisionality, with R_{ref} in [m], n_{ref} in [m^{-3}] and T_{ref} in [eV]. It is assumed that each species collisionality is calculated in the code consistently with the species input parameters (i.e. the normalised species temperature and density are used to calculate the collisionality of each species). This behaviour can be altered by specific collisionality switches described in Sec. **??**.

3.6.2 Switches

- Pitch angle scattering only is retained (as opposed to pitch angle and energy scattering)
- Electron-ion collisions only are retained (as opposed all interspecies collisions)
- Enhancement factor for electron to (main) ion collisions. This is typically used to mimic the impact of impuritites on the electron-ions collisions.
- Is momentum conservation ensured?
- Is energy conservation ensured?
- Are FLR retained in the collision treatment?

Note that the implementation of collisions is highly code dependent and the list above does not give a complete characterisation of how collisions were treated in the run. Jpwever, this information can be retrieved from the specific code input file used for the run, which is also stored in the database, and the code documentation,

3.6.3 Summary of the collision parameters

Name	Value/Range	Type	Dimension
collisionality	≥ 0	Real	1
pitch_only_flag	0 or 1	Logical	1
ei_collisions_only_flag	0 or 1	Logical	1
collisions_enhancement	≥ 1	Real	1
momentum_conservation_flag	0 or 1	Logical	1
energy_conservation_flag	0 or 1	Logical	1

3.7 Other switches

- Are the centrifugal effects included?
- Initial value run or eigenvalue solver? -¿ move to the mode section?

Chapter 4

Outputs

4.1 Mode amplitude

In linear runs, unstable modes are exponentially growing in time and so are the associated fluxes. The exponentially growing outputs stored in the database are therefore normalised to a dimensionless mode amplitude defined as:

$$A_f(k_x,k_y)(t) = \sqrt{\int \left[|\hat{\phi}_N(k_x,k_y,\theta)|^2 + |\hat{A}_{\parallel N}(k_x,k_y,\theta)|^2 + |\hat{B}_{\parallel} N(k_x,k_y,\theta)|^2\right] \mathrm{d}\theta} \tag{4.1}$$

with the Fourrier components of the electrostatic potential and vector potential normalised as follows:

$$\hat{\phi}_N = \frac{1}{\rho_*}\frac{q_{\mathrm{ref}}}{T_{\mathrm{ref}}}\hat{\phi} \qquad \hat{A}_{\parallel N} = \frac{1}{\rho_*^2}\frac{1}{L_{\mathrm{ref}}B_{\mathrm{ref}}}\hat{A}_{\parallel} \qquad \hat{B}_{\parallel N} = \frac{1}{\rho_*}\frac{1}{B_{\mathrm{ref}}}\hat{B}_{\parallel} \tag{4.2}$$

where $\rho_* = \rho_{\mathrm{ref}}/L_{\mathrm{ref}}$. The value of the mode amplitude in a linear run has little meaning by itself and is not stored in the database.

4.2 Mode growth rate and frequency

The normalisations of the mode growth rate γ and frequency ω_r are:

$$\gamma_N(k_x,k_y) = \gamma(k_x,k_y)\frac{L_{\mathrm{ref}}}{v_{\mathrm{thref}}} \qquad \text{and} \qquad \omega_{rN}(k_x,k_y) = \omega_r(k_x,k_y)\frac{L_{\mathrm{ref}}}{v_{\mathrm{thref}}} \tag{4.3}$$

By convention, unstable modes have a positive growth rate and modes propagating in the ion diamagnetic drift direction have a positive frequency (and therefore a negative frequency when they are propagating in the electron diamagnetic drift direction).

For initial value runs, the following (post-processing) method is used to determine the tolerance on the run convergence:

$$\gamma_{\mathrm{tol}} = \sqrt{\frac{1}{\Delta t}\int_{t-\Delta t}^{t} \gamma^2(t)\,\mathrm{dt}}$$

where $\Delta t \sim 1/\gamma$ and

$$\gamma(t) = \frac{1}{\delta t}[\ln A_f(t) - \ln A_f(t-\delta t)]$$

with δt depending on the code setup but in any case several times smaller than Δt. Note that any exponentially growing quantity can be used in place of $A_f$to compute the time dependent growth rate..

4.2.1 Summary of the eigenvalue outputs

Name	Value/Range	Type	Dimension
growth_rate	-	Real	N_{modes}
tolerance_growth_rate	$0 < \gamma_{\text{tol}} \leq 0.1$	Real	1
frequency	-	Real	N_{modes}

For initial value runs, $N_{\text{modes}} = 1$ and only the linear outputs corresponding to the most unstable run are given. When the eigenvalue solver is used N_{modes} indicates the number of modes for which the linear outputs are given.

4.3 Parallel mode structure

4.3.1 Parallel grid

The variation of the mode amplitude and phase in the parallel direction is given as a function of the poloidal angle θ defined previously.

4.3.2 Perturbed electrostatic potential

$$\phi_{Nf}(\theta) = \frac{\hat{\phi}_N(k_x, k_y, \theta)}{A_f(k_x, k_y)} \mathrm{e}^{i\alpha}$$

The phase factor α is chosen so that the imaginary part of ϕ_{Nf} is zero at $\theta = 0$ which makes comparisons of the mode structure between different runs easier.

4.3.3 Perturbed parallel vector potential (magnetic field flutter)

$$A_{\parallel Nf}(\theta) = \frac{\hat{A}_{\parallel N}(k_x, k_y, \theta)}{A_f(k_x, k_y)} \mathrm{e}^{i\alpha}$$

4.3.4 Perturbed parallel magnetic field (magnetic field compression)

$$B_{\parallel Nf}(\theta) = \frac{\hat{B}_{\parallel N}(k_x, k_y, \theta)}{A_f(k_x, k_y)} \mathrm{e}^{i\alpha}$$

4.3.5 Moments of the distribution function

It may be interesting to add as an optional output the gyro-averaged moments of the distribution function. To be discussed.

4.3.6 Summary of the parallel outputs

Name	Value/Range	Type	Dimension
poloidal_angle	$-N_p\pi$ to $N_p\pi$	Real	$N_{\text{pol grid}}$
phi_potential_perturbed	-	Real	$N_{\text{pol grid}} \times N_{\text{modes}}$
a_parallel_perturbed	-	Real	$N_{\text{pol grid}} \times N_{\text{modes}}$
b_field_parallel_perturbed	-	Real	$N_{\text{pol grid}} \times N_{\text{modes}}$

4.4 Gyro-center fluxes

4.4.1 Definition

For each species, the flux-surface averaged contravariant radial component of the particle flux, energy flux and toroidal angular momentum flux are given by:

$$\Gamma_s = \left\langle \int f_s \left[\mathbf{v}_\mathbf{E} + \mathbf{v}_{\mathbf{B}_\perp} + \mathbf{v}_{\nabla B_\parallel}\right] \cdot \nabla r \, \mathrm{d}\mathbf{v} \right\rangle \tag{4.4}$$

$$\Pi_s = \left\langle \int m_s R \frac{B_t}{B} v_\parallel f_s \left[\mathbf{v}_\mathbf{E} + \mathbf{v}_{\mathbf{B}_\perp} + \mathbf{v}_{\nabla B_\parallel}\right] \cdot \nabla r \, \mathrm{d}\mathbf{v} \right\rangle \tag{4.5}$$

$$Q_s = \left\langle \int \frac{1}{2} m_s v^2 f_s \left[\mathbf{v}_\mathbf{E} + \mathbf{v}_{\mathbf{B}_\perp} + \mathbf{v}_{\nabla B_\parallel}\right] \cdot \nabla r \, \mathrm{d}\mathbf{v} \right\rangle \tag{4.6}$$

where f_s is the perturbed guiding center distribution function of species s and the two terms on the right hand side correspond to the fluxes induced by the electrostatic, magnetic flutter and magnetic compression drifts:

$$\mathbf{v}_\mathbf{E} = \frac{\mathbf{b} \times \nabla \left\langle \phi \right\rangle_{\mathrm{gy}}}{B} \qquad \mathbf{v}_{\mathbf{B}_\perp} = -v_\parallel \frac{\mathbf{b} \times \nabla \left\langle A_\parallel \right\rangle_{\mathrm{gy}}}{B} \qquad \mathbf{v}_{\nabla B_\parallel} = \frac{\mu}{Ze} \frac{\mathbf{b} \times \nabla \left\langle B_\parallel \right\rangle_{\mathrm{gy}}}{B} \tag{4.7}$$

with $\left\langle \phi \right\rangle_{\mathrm{gy}}$, $\left\langle A_\parallel \right\rangle_{\mathrm{gy}}$ and $\left\langle B_\parallel \right\rangle_{\mathrm{gy}}$, the gyro-averaged perturbed electrostatic potential, parallel vector potential and parallel magnetic field, respectively.

Note that the momentum flux in the expression above only includes the toroidal projection of the parallel momentum. The toroidal projection of the perpendicular momentum also contributes to the total momentum flux, see e.g. [7]. This contribution is not included here but could be added in the future.

4.4.2 Laboratory frame versus rotating frame

To describe inertial effects associated with the background rotation, several gyrokinetic codes (e.g. GKW, GENE, GS2) solve the gyro-kinetic equation in the frame rotating as a rigid body with the angular frequency ω_Φ. The Laboratory frame fluxes are of course the relevant ones for comparison with the experiments. They can be computed from quantities expressed in the rotating frame as follows:

$$\Gamma_s^{\mathrm{L}} = \Gamma_s^{\mathrm{co}} \tag{4.8}$$

$$\Pi_s^{\mathrm{L}} = \Pi_s^{\mathrm{co}} + \left\langle \int m_s \omega_\Phi \left(\frac{R B_t}{B}\right)^2 f_s \mathbf{v}_\chi \cdot \nabla r \, \mathrm{d}\mathbf{v} \right\rangle \tag{4.9}$$

$$Q_s^{\mathrm{L}} = Q_s^{\mathrm{co}} + \omega_\Phi \Pi_s^{\mathrm{co}} + \left\langle \int \frac{1}{2} m_s (R\omega_\Phi)^2 f_s \mathbf{v}_\chi \cdot \nabla r \, \mathrm{d}\mathbf{v} \right\rangle \tag{4.10}$$

with $\mathbf{v}_\chi = \mathbf{v}_\mathbf{E} + \mathbf{v}_{\mathbf{B}_\perp} + \mathbf{v}_{\nabla B_\parallel}$ and all the expressions in the right hand sides evaluated in the rotating frame. For convenience, both the Laboratory frame and rotating frame fluxes are stored in the database.

4.4.3 Normalisation

The fluxes are given for each Fourier mode, normalised to the corresponding (linear) mode amplitude and made dimensionless as follows:

$$\Gamma_{Ns}(k_x, k_y) = \frac{1}{A_f} \frac{\Gamma_s(k_x, k_y)}{n_{\mathrm{ref}} v_{\mathrm{thref}} \rho_*^2} \tag{4.11}$$

$$\Pi_{Ns}(k_x, k_y) = \frac{1}{A_f} \frac{\Pi_s(k_x, k_y) \mathcal{V}'}{n_{\mathrm{ref}} m_{\mathrm{ref}} L_{\mathrm{ref}} v_{\mathrm{thref}}^2 \rho_*^2} \tag{4.12}$$

$$Q_{Ns}(k_x, k_y) = \frac{1}{A_f} \frac{Q_s(k_x, k_y) \mathcal{V}'}{n_{\mathrm{ref}} T_{\mathrm{ref}} v_{\mathrm{thref}} \rho_*^2} \tag{4.13}$$

In addition, the electrostaticm magnetic flutter and magnetic compressions are stored separately (e.g. $\Gamma_{Ns} = \Gamma_{Ns,\phi} + \Gamma_{Ns,A_\parallel} + \Gamma_{Ns,B_\parallel}$) for each flux.

4.4.4 Summary of the fluxes outputs

Name	Value/Range	Type	Dimension
particle_phi_potential_lab_frame	-	Real	$N_{\text{species}} \times N_{\text{modes}}$
particle_a_parallel_lab_frame	-	Real	$N_{\text{species}} \times N_{\text{modes}}$
particle_b_field_parallel_lab_frame	-	Real	$N_{\text{species}} \times N_{\text{modes}}$
momentum_phi_potential_lab_frame	-	Real	$N_{\text{species}} \times N_{\text{modes}}$
momentum_a_parallel_lab_frame	-	Real	$N_{\text{species}} \times N_{\text{modes}}$
momentum_b_field_parallel_lab_frame	-	Real	$N_{\text{species}} \times N_{\text{modes}}$
heat_phi_potential_lab_frame	-	Real	$N_{\text{species}} \times N_{\text{modes}}$
heat_a_parallel_lab_frame	-	Real	$N_{\text{species}} \times N_{\text{modes}}$
heat_b_field_parallel_lab_frame	-	Real	$N_{\text{species}} \times N_{\text{modes}}$
momentum_phi_potential_co_frame	-	Real	$N_{\text{species}} \times N_{\text{modes}}$
momentum_a_parallel_co_frame	-	Real	$N_{\text{species}} \times N_{\text{modes}}$
momentum_b_field_parallel_co_frame	-	Real	$N_{\text{species}} \times N_{\text{modes}}$
heat_phi_potential_co_frame	-	Real	$N_{\text{species}} \times N_{\text{modes}}$
heat_a_parallel_co_frame	-	Real	$N_{\text{species}} \times N_{\text{modes}}$
heat_b_field_parallel_co_frame	-	Real	$N_{\text{species}} \times N_{\text{modes}}$

Chapter 5

Meta-data

Chapter 6

Test cases

6.1 Test 1

A simple electrostatic test case close to the GA standard case with kinetic electrons.

6.1.1 Species

Species	Z_{sN}	m_{sN}	n_{sN}	T_{sN}	L_{ref}/L_{n_s}	L_{ref}/L_{T_s}	u_{sN}	u'_{sN}
e	-1	2.7232×10^{-4}	1	1	3	9	0	0
D	1	1	1	1	3	9	0	0

6.1.2 Magnetic equilibrium

r_N	R_{0N}	q	$\hat{s}$	s_b	s_j	β'_N
0.16	1	2	1	1	1	0

α_0	α_1	α_2	α_3	α_4	α_5	α_6	β_1	β_2	β_3	β_4	β_5	β_6
0.16	0	0	0	0	0	0	0	0	0	0	0	0

α'_0	α'_1	α'_2	α'_3	α'_4	α'_5	α'_6	β'_1	β'_2	β'_3	β'_4	β'_5	β'_6
1.0	0	0	0	0	0	0	0	0	0	0	0	0

6.1.3 Modes

$k_{\theta *}\rho_{\mathrm{ref}}$	0.2	0.4	0.6	0.8
$k_{r *}\rho_{\mathrm{ref}}$	-0.2	0	0.2	

6.1.4 Collisionality and beta

β_{eN}	ν_N
0	0

6.2 Test 2

Same with shaping.

6.2.1 Species

Species	Z_{sN}	m_{sN}	n_{sN}	T_{sN}	L_{ref}/L_{n_s}	L_{ref}/L_{T_s}	u_{sN}	u'_{sN}
e	-1	2.7232×10^{-4}	1	1	3	9	0	0
D	1	1	1	1	3	9	0	0

6.2.2 Magnetic equilibrium

r_N	R_{0N}	q	$\hat{s}$	s_b	s_j	β'_N
0.5	1	2	1	1	1	0.03

α_0	α_1	α_2	α_3	α_4	α_5	α_6	β_1	β_2	β_3	β_4	β_5	β_6
0.5831	-0.0242	-0.0987	0.0321	0.0174	-0.0107	-0.0020	0	0	0	0	0	0

α'_0	α'_1	α'_2	α'_3	α'_4	α'_5	α'_6	β'_1	β'_2	β'_3	β'_4	β'_5	β'_6
1.2898	-0.3984	-0.3892	0.2734	0.1136	-0.1085	-0.0097	0.2892	0.0195	-0.0417	0.0153	0.0140	-0.0065

6.2.3 Modes

$k_{\theta *}\rho_{\mathrm{ref}}$	0.2	0.4	0.6	0.8
$k_{r *}\rho_{\mathrm{ref}}$	-0.2	0	0.2	

6.2.4 Collisionality and beta

β_{eN}	ν_N
0	0

Bibliography

[1] O. Sauter and S.Yu. Medvedev. *Comput. Phys. Comm.*, 184:293, 2013.

[2] F.L. Hinton and R.D. Hazeltine. *Rev. Mod. Phys.*, 48:239, 1976.

[3] S.P. Hirshman and D.J. Sigmar. *Nucl. Fusion*, 21:1079, 1981.

[4] Y. Camenen *et al. Phys. Plasmas*, 23:022507, 2016.

[5] J. Candy. *Plasma Phys. Control. Fusion*, 51:105009, 2009.

[6] G. Merlo, O. Sauter, *et al. Phys. Plasmas*, 23:032104, 2016.

[7] B. Scotta and J. Smirnov. *Phys. Plasmas*, 17:112302, 2010.